12-13-2018

Graphene Plasmonics: A Platform for 2D Optics

Yuancheng Fan
Northwestern Polytechnical University

Nian-Hai Shen
Iowa State University and Ames Laboratory, nhshen@ameslab.gov

Fuli Zhang
Northwestern Polytechnical University

Qian Zhao
Tsinghua University

Hongjing Wu
Northwestern Polytechnical University

See next page for additional authors

Graphene Plasmonics: A Platform for 2D Optics

Abstract
2D optics is gradually emerging as a frontier in modern optics. Plasmons in graphene provide a prominent platform for 2D optics in which the light is squeezed into atomic scale. This report highlights some recent progresses in graphene plasmons toward the 2D optics. The launch, observation, and advanced manipulation of propagating graphene plasmons for 2D optical circuits are described. Representative achievements associated with graphene metasurfaces, challenges, recent progresses like photoexcited graphene metasurfaces, and the transformation optics linking 2D to bulk optics with singularity are investigated.

Keywords
graphene plasmons, 2D optics, optical circuits, tunable metamaterials, terahertz, infrared, surface conductivity

Disciplines
Optics

Authors
Yuancheng Fan, Nian-Hai Shen, Fuli Zhang, Qian Zhao, Hongjing Wu, Quanhong Fu, Zeyong Wei, Hongqiang Li, and Costas M. Soukoulis

DOI: 10.1002/ ((please add manuscript number))
Article type: Progress Report

Graphene Plasmonics: A Platform for Two-Dimensional Optics

Yuancheng Fan, Nian-Hai Shen, Fuli Zhang, Qian Zhao, Hongjing Wu, Quanhong Fu, Zeyong Wei, Hongqiang Li, and Costas M. Soukoulis*

Prof. Y. Fan, Prof. F. Zhang, Prof. H. Wu, Dr. Q. Fu
Key Laboratory of Space Applied Physics and Chemistry, Ministry of Education and Department of Applied Physics, School of Science, Northwestern Polytechnical University, Xi'an 710129, China
E-mail: phyfan@nwpu.edu.cn
Dr. N.-H. Shen, Prof. C. M. Soukoulis
Ames Laboratory and Department of Physics and Astronomy, Iowa State University, Ames, Iowa 50011, United States
Prof. Q. Zhao
State Key Laboratory of Tribology, Department of Mechanical Engineering, Tsinghua University, Beijing 100084, China
Prof. Z. Wei, Prof. H. Li
Key Laboratory of Advanced Micro-structure Materials (MOE) and School of Physics Science and Engineering, Tongji University, Shanghai 200092, China
Prof. C. M. Soukoulis
Institute of Electronic Structure and Laser, FORTH, 71110 Heraklion, Crete, Greece

Abstract: Two-dimensional (2D) optics is gradually emerging as the frontier in modern optics. Plasmons in graphene provide a prominent platform for two-dimensional optics in which the light is squeezed into an atomic scale. This paper highlights some recent progresses in graphene plasmons towards the 2D optics. The launching, observation, and advanced manipulations of propagating graphene plasmons for 2D optical circuits are described. Representative achievements associated with graphene metasurfaces, challenges, recent progresses like photoexcited graphene metasurfaces and transformation optics linking 2D to bulk optics with singularity are investigated.

Keywords: graphene plasmons, 2D optics, optical circuits, tunable metamaterials, terahertz, infrared, surface conductivity

1. Introduction

Graphene has been intensively studied for applications in nanoelectronics and nanophotonics.[1-5] It has stimulated intensive studies in two-dimensional (2D) materials [6-8] since the first exfoliation from graphite by Geim and Novoselov.[9] There have been numerous reports regarding the advantages of graphene, which is fascinating for applications in nanoelectronics due to its high mechanical strength,[10] electronic mobility,[11] and thermal conductivity.[12] Graphene also has been extensively investigated aiming toward potential applications in advanced photonics.[13-17] Graphene supports stronger bonding of surface plasmons,[18-29] and the Dirac fermions provides large tunabilities in optical response via magnetic field, electrostatic field, and doping in ultra-wide bands.[30-33] Compared to the conventional plasmonic materials—noble metals, the plasmonic resonance of graphene resides in the technically important bands: terahertz and infrared frequencies.[15, 34-49] Graphene plasmons show much stronger confinement of light compared to that in noble metals. The light is localized in the vicinity of the atomic thin film, providing a novel platform to manipulate light in a 2D manner. It had been shown that the propagation of plasmons can be freely controlled in graphene sheet.[32]

Furthermore, the localized surface plasmon resonances in structured graphene (such as graphene islands) demonstrate stronger field confinement around the edge of graphene particles and provide more flexible and complex manipulation to the light fields.[50-59] Graphene sheet can be patterned into rationally designed micro/nano-structures as atomically thin metasurfaces, with which, significantly enhanced light-graphene interactions have been demonstrated. Metamaterials,[60-73] formed by tailored subwavelength building blocks, serve as a promising platform for versatile manipulation of light by exploiting the excitations of plasmonic resonances and Mie resonances. Metamaterials made of a single or a few planar layers, named as metasurfaces,[74-81] have attracted particular interests in light manipulation. Considering the physical dimension of materials, the realistic 2D material—graphene is with natural connection to artificial 2D materials—metasurface. Moreover, mutual promotions can be achieved by exploiting graphene metasurfaces: i) replacing conventional plasmonic materials—noble metals with graphene will provide frequency-agile responses for local resonant metasurfaces; and the elements of graphene metasurface possess superior subwavelength property, which shall greatly benefit various applications in wavefront engineering. ii) one can get the significantly enhanced light-graphene interactions in graphene metasurfaces. Various graphene-based metasurfaces have been investigated experimentally and theoretically for functional manipulations of terahertz and infrared light,[82-104] including high-performance absorber, cloaking, polarization control, wavefront engineering, sensing, nonlinear optics and lasing.

In studying optical properties of graphene, it is generally modeled with a frequency-dependent dynamic conductivity under the random-phase-approximation (RPA).[105-107] The model takes into account both contributions from intraband and interband transitions. The surface conductivity is associated to the doping level of graphene, or the Fermi energy away from Dirac point. The conductivity can be significantly tuned by shifting the Fermi energy via electric field, magnetic field, and chemical doping.[30-31, 33, 84, 93, 108] Both the propagating and localized graphene plasmons are beneficial for dynamical control of optical signals on a surface, providing a platform for ***2D optics***. However, there are still many challenging aspects in developing practical 2D optical components and systems based on graphene plasmonics. These include: i) the weak light-graphene coupling and the intrinsic loss in graphene significantly limits the performance of optical devices based on graphene, so, to enhance the light-matter interaction in graphene is of fundamental importance to take further advantage of graphene based 2D plasmonic devices and systems. ii) designing methods for 2D optical components based on graphene plasmons have been seldomly studied compared to that in bulk optics. The development of efficient strategies for this task is essential for myriad applications based on the 2D surface plasmon excitations in graphene.

The review will show some state-of-the-art research activities in the field of graphene based 2D optics including 2D optical circuits with propagating graphene plasmons and graphene metasurfaces with properly excited localized graphene plasmons. We will also present perspectives and challenges in future applications of graphene based 2D optics. Though we mainly focus on the graphene, it should be noted that space restrictions force us to leave out many other optical researches on 2D materials beyond graphene that relate to 2D optics concepts. For the advances regarding other 2D materials beyond graphene in this fast-developing field, the readers can refer to some specific literature focusing on the related topics.

2. Propagating graphene plasmons: 2D optical circuits

Surface plasmon mode at the interface of metal and dielectric is promising in manipulating light waves with wavelengths much smaller than that in free space, which enables subwavelength optics for nanophotonic devices.[109-110] The optical fields can be highly confined and guided in the vicinity of metal-dielectric interface especially at visible spectrum. However, the weak confinement and increased losses at lower frequencies make plasmons in noble metals less attractive for terahertz and mid-infrared applications.[15] As discussed above, the intraband transition contribution of graphene on its surface conductivity is similar to that of plasmonic metals, and the plasma frequency of graphene can be freely tuned via various dopings. The carriers in doped graphene can be excited collectively, similar to the plasmonic oscillations in noble metals. The simplest dielectric/graphene/dielectric structure supports TM plasmons. The plasmon dispersion of a graphene film follows the general relation of 2D systems, i.e., $\omega_{pl}\left(q\right)\propto\sqrt{q}$. Considering the realistic carrier concentration in graphene, the plasmon frequency of graphene lies in the terahertz and infrared regime. Comparing to the plasmons in noble metals, the graphene plasmons present many appealing properties including: i) Strong confinement of optical fields within the atomic scale around graphene sheet, providing a new platform for nonlinear plasmonics and sensitive biosensing applications; ii) Significantly tunable plasmonic response, originating from its strong dependence on the Fermi energy relative to the Dirac point, and such a property is very useful in achieving active plasmonic optics.

2.1. Fundamental properties and observation of the propagating graphene plasmons

Pioneering theoretical work by Mikhailov and Ziegler predicted that there exists a transverse electric mode in graphene due to the unique linear "relativistic" spectrum of charge carriers.[19] Jablan *et al.* studied plasmons in doped graphene using RPA and number-conserving relaxation-time approximation with experimentally available graphene parameters. They showed that it is possible to realize strong wave localization and low losses simultaneously under sufficiently large doping at frequencies below the optical phonon mode. Although the collective surface charge oscillation in graphene is similar to surface plasmons in metals, it is noted that the plasmon in graphene is 2D collective excitations. Since electrons in graphene are localized in the transverse dimension,[111] and the unique electronic dispersion in graphene (linear Dirac dispersion) leads to essentially different dispersions of plasmons,[18] it would be divertive to experimentally excite and measure the propagating graphene plasmons. It has been reported some measurements of the plasmon dispersion in graphene films with electron energy loss spectroscopy (EELS) technique, in cases of monolayer graphene and multilayer graphene positioned on a SiC wafer and on a copper film by chemical vapor deposition (CVD).[112-113]

Later, a kind of developed scanning near-field optical microscopy (SNOM), namely the scattering-type SNOM was employed for direct launching and imaging the high-*q* graphene plasmons.[21-22] The diagram of the nano-imaging is illustrated in **Figure 1a**.[21] In the experimental setup, the acuate tip (radius of curvature: 25 nm) of an atomic force microscope (AFM) is irradiated with a focused beam. The spatial resolution of scattering-type SNOM is proved to be far smaller than the plasmon wavelength of graphene. From the scattering amplitude, the electric field force inside the nano-gap can then be directly demonstrated. It is not necessary to fabricate specialized periodic structures within the scattering-type SNOM technique. A frequency ω = 892 cm^{-1} accordant to a wavelength of 11.2 μm in the infrared regime was set to study undeviatingly the characteristics of graphene plasmons. **Figures 1b–e** indicate the nano-imaging results at the graphene–SiO2 interface, the boundary between different layered graphenes, around point and circular defects, and strongly tapered corners of graphene respectively. In all these cases, a periodicity of around 100 nm is observed of the fringe patterns, confirming that the graphene plasmon has a wavelength of 200 nm.

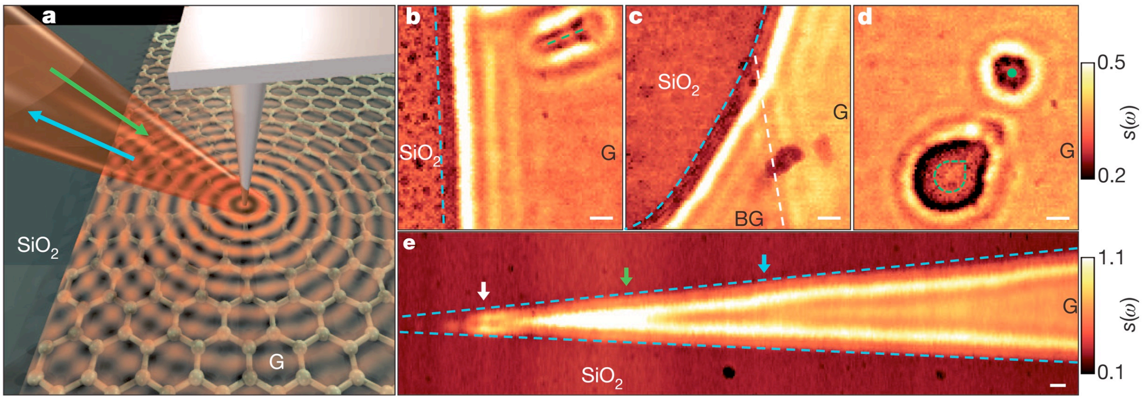

Figure 1. a) Diagram of an infrared nano-imaging experiment at the surface of graphene on SiO_2. Green and blue arrows display the directions of incident and back-scattered light, respectively. Concentric red circles illustrate plasmon waves launched by the illuminated tip. b-e) Images of infrared amplitudes (ω = 892 cm^{-1}) defined in the text taken at zero gate voltage. These images show a characteristic interference pattern close to graphene edges (blue dashed lines) and defects (green dashed lines and green dot), and at the boundary between single and bilayer graphene (white dashed line). Locations of boundaries and defects were determined from AFM topography taken simultaneously with the near-field data. Scale bars, 100 nm. All data were acquired at ambient conditions. Reproduced with permission. [21] Copyright 2012, Nature Publishing Group.

Chen *et al.* demonstrated the launch and detection of propagating optical plasmons in tapered graphene nanostructures using near-field scattering microscopy with infrared excitation light.[22] In the study, real-space images of the extreme subwavelength graphene plasmon are directly captured. Strong optical field confinement turns a graphene nanostructure into a tunable resonant plasmonic structure with extremely tiny mode volume and the subwavelength sized resonance can then be controlled in situ by doping the graphene. Complete switching of the resonant plasmonic modes is implemented for a graphene-based optical transistor. The local density of optical states (LDOS) maps were theoretically computed to understand the underlying mechanisms of the observed resonant optical modes and the interference fringes in the tapered graphene nanostructures. The calculated LDOS maps (**Figure 2a**) demonstrate interference fringes parallel to the graphene edge and localized fields around the tip. The high consistency between experiment and theory confirms that the plasmon interference originated from plasmon reflections at the graphene margins leads to the fringes in the broader part of the ribbon.

Phase-resolved scattering-type SNOM technique was developed by Gerber *et al.* to retrieve the complete amplitude and phase information via spatially resolved image of graphene plasmons.[23] In the setup, the tip-scattered field is enhanced at the HgCdTe detector (Kolmar Technologies) with the background signal of the Michelson interferometer with beam-splitter. The abundant complete tip-scattered near field can be measured accurately by gathering raster-scanned imaging for orthogonal reference phases. The experimental setup was used to investigate the discrete and reflected surface plasmon polaritons (SPPs) by interruptions such as margins, defects, and grain boundaries, providing nanoscale perspective for the study of local electronic structure and dynamics in graphene. **Figure 2b** shows the AFM photo, near-field amplitude, and phase in an area of monolayer graphene with grain boundaries and folds.

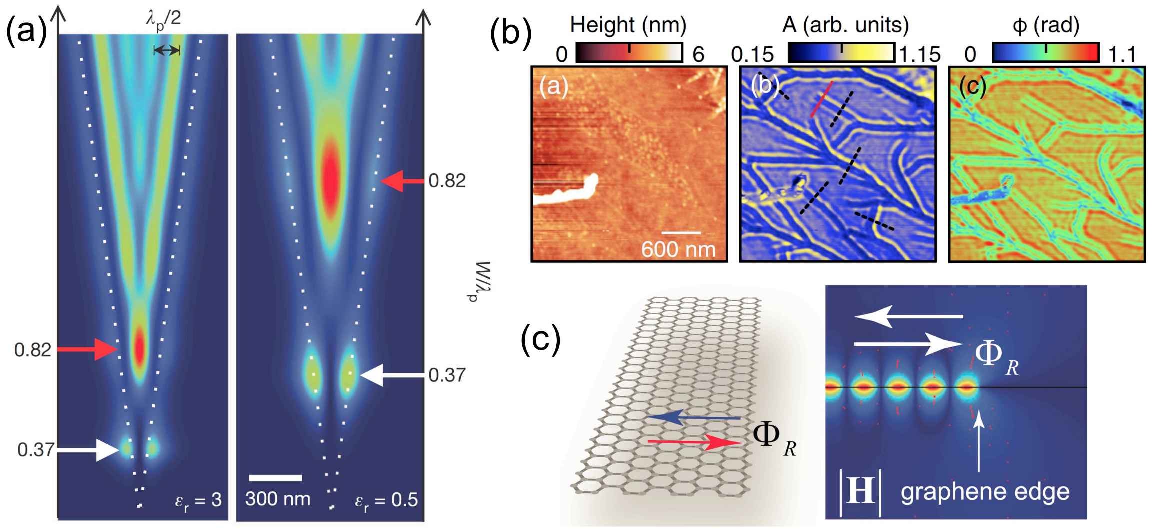

Figure 2. a) Spatial distribution of the LDOS calculated for homogeneous ribbons with increasing width (from bottom to top), supported on a dielectric with relative permittivity 3 (left) or 0.5 (right). The ribbon width of the two lowest-order modes is shown in units of the plasmon wavelength of extended graphene. b) From left to right: AFM topography, near-field amplitude, and near-field phase of a region of single-layer graphene with a high concentration of grain boundaries and folds. c) Left: Schematic of the reflection of a graphene plasmon by an edge. A graphene plasmon propagating from left to right (shown by a red arrow) acquires a phase Φ_R and then propagates back (which is shown by a blue arrow). Right: Computed absolute value of the magnetic field created by the interference between the incident graphene plasmon and that reflected from the edge. a) Reproduced with permission.[22] Copyright 2012, Nature Publishing Group. b) Reproduced with permission.[23] Copyright 2014, American Physical Society. c) Reproduced with permission.[114] Copyright 2014, American Physical Society.

The investigation on the propagation and scattering of graphene plasmons in finite-sized of graphene domains with edges or boundaries is rather insufficient. Distinct features compared to that of bulk or 3D optics is expected. For instance, recently Nikitin *et al.* demonstrated an anomalous reflected phase of graphene plasmon at the boundary (**Figure 2c**).[114] Launching of propagating plasmons in a controlled manner is another important issue for 2D nanophotonics applications. Apart from the scattering-type SNOM based excitation of graphene plasmons, some different methods were proposed for launching and controlling propagating graphene plasmons: asymmetric surface plasmon dispersion caused by a magneto-optical substrate was proposed by Liu *et al.* for directional excitation of graphene plasmons. The direction of launching can be manipulated by gating the graphene layer with electricity.[115] Wang *et al.* demonstrated that a circularly polarized dipole and two mirror image symmetric dipoles with orthogonally polarizations can be properly controlled for directional generation of propagating graphene plasmons.[116] Vantasin *et al.* found that a monolayer graphene nanoridge with no foreign objects, can support standing SPP waves. And with double-nanoridge system and wavelength-sorted launching, unidirectional SPP excitation of graphene plasmons can be demonstrated with normal illumination with linear polarization.[117] Constant *et al.* illustrated that the generation of graphene plasmons can be accomplished without local scatters by manipulating the phase matching conditions.[118] Recently, significant progresses have been achieved in experiments: i) Ballistic graphene plasmon at low temperatures was investigated using nano-scale infrared imaging and an intrinsic propagation length up to 50 plasmonic wavelengths was experimentally observed;[119-120] ii) Graphene acoustic plasmons modes[121] have been demonstrated to have confinement down to the length scale of single atom.[122] All these fundamental studies and progresses on the graphene plasmon excitations strongly support advanced manipulations on the graphene plasmons towards functional applications.

2.2. Wavefront engineering of the propagating graphene plasmon

The tunable graphene plasmon was proposed for wavefront engineering in a flake of graphene. A study theoretically showed that, by designing and manipulating spatially inhomogeneous, non-uniform conductivity patterns across a flake of graphene, one can achieve one-atom-thick infrared metamaterials and transformation optical devices.[32] A 2D waveguide consisting of three different regions on the atomic thick graphene was designed (**Figure 3a**, left panel). And one step further, an IR splitter, according to the waveguide notion, was accomplished with suitable conductivity patterns plan on the graphene, generated, for example, using rugged ground plane or other techniques to produce indispensable spatial distribution of the biased electric field (see **Figure 3a**, right panel). The inhomogeneous conductivity patterning can be realized with different techniques, such as using uneven ground plane, fabricating non-uniform dielectric spacers, and applying gate electric or magnetic field.

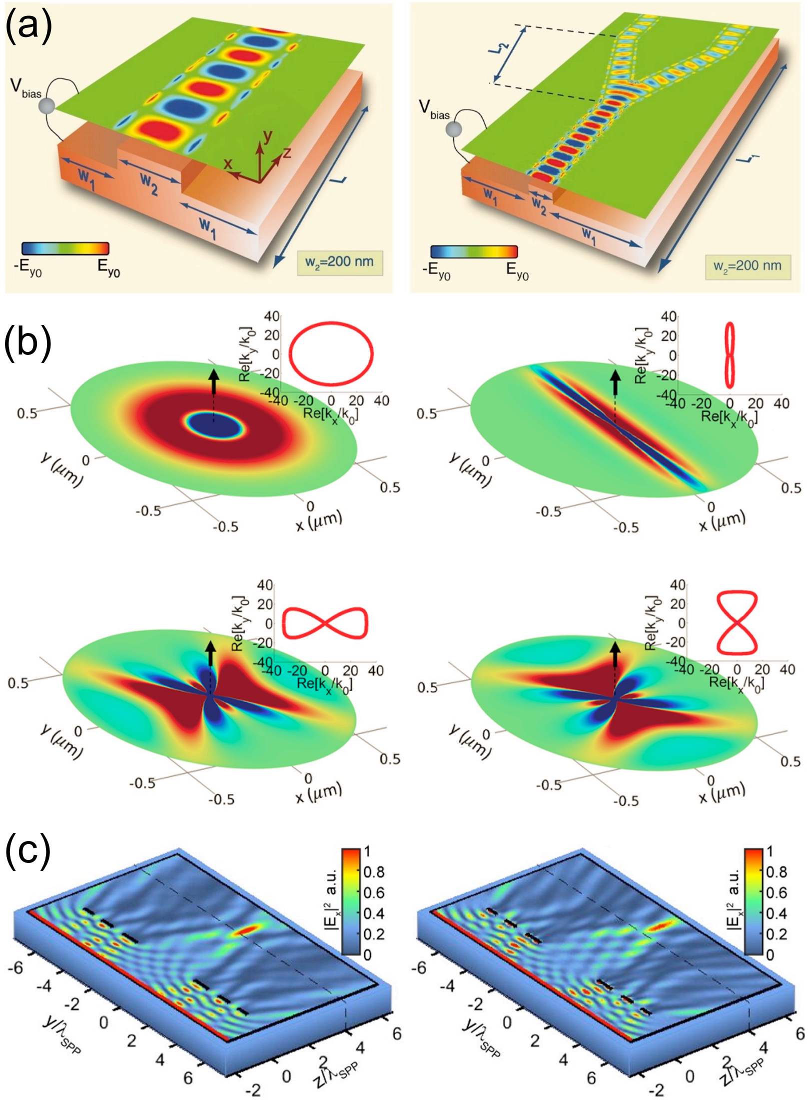

Figure 3. a) Simulation results of electric field for an IR-guided wave at 30 THz along the ribbon-like section of graphene (left) and the ribbon-like section splits into two paths (right). Different scale bars in each panel. b) SPP excitation along homogeneous uniaxial metasurfaces by a *z*-oriented dipole emitter (represented by a black arrow) located at a distance of 10 nm above the surface. The 2D plots show the E_z field component of propagating SPPs. The insets present the corresponding isofrequency contour. Top left: Isotropic metasurface. Top right: Extremely anisotropic conductive-near-zero metasurface. Bottom: Hyperbolic metasurfaces. c) Surface plot of the intensity pattern on the 2D-sheet demonstrating SPP focusing at the desired focal spot calculated using effective model (left) and the intensity pattern calculated using COMSOL for the three-dimensional structure with actual holes for comparison. The focal spot shifted due to the additional phase difference (π) added by the holes. a) Reproduced with permission.[32] Copyright 2011, AAAS. b) Reproduced with permission.[123] Copyright 2015, American Physical Society. c) Reproduced with permission.[124] Copyright 2016, American Chemical Society.

In addition to this spatial nonuniform conductivity route for engineering the wavefront of graphene plasmon, various novel mechanisms were also proposed, including the wavefront engineering with phase transition in anisotropic graphene sheet and distributed in-plane or out-of-plane scatters that modulate the amplitude and phase of propagating graphene plasmons. The concept of ultrathin hyperbolic and extremely anisotropic conductive sheet, which allows strong light-matter interactions while providing extreme field confinement, was introduced for the control of 2D plasmons for their novel dispersion relation (see **Figure 3b**).[123] And these properties were suggested to be realized in extremely anisotropic planar hyperlens obtained with proper adjustment to the conductivity of a uniform 2D graphene.

It is found that the propagating features of SPPs in 2D sheets like structured graphene films can be made similar to the guiding of plane waves in consubstantial layers with slight out-of-plane scattering.[124] With the use of reflection, refraction, diffraction, and also generalized refraction laws analogous to plane waves, it is achievable to control the in-plane propagation of surface waves. For example, the 2D SPPs in a hole drilled homogeneous 2D-sheet was studied for focusing. **Figure 3c** demonstrates the intensity pattern of a hole system with properly designed lateral dimensions. Graphene plasmons concentrate light in a region of atomic scale, suggesting the possibility of using graphene plasmons for the construction of true 2D photonic circuits.

3. Localized graphene plasmonics: 2D metasurfaces

Renewed interest in graphene plasmons has come from recent advances in producing large scale graphene films and graphene based micro/nanostructured materials. One of the most attractive aspects of the collective excitations in structured graphene is the *in situ* much stronger concentrated light and the significantly enhanced modulation of the reflection, transmission, and absorption spectra in comparison to that of a homogenous sheet. The realization of 2D micro/nanostructures by patterning graphene films into periodic arrays provides opportunities in manipulating light with atomically thin sheets, and exploiting tunable graphene plasmon resonances.

Plasmonic metamaterials composing subwavelength-sized elements are promising for the manipulation of light on a subwavelength scale. A special class of metamaterials made of a single or few layers, named as metasurfaces, has been studied from various perspectives in recent years to explore novel light manipulation capabilities. The meta-surface is with natural connection to graphene in the view of following aspects: i) replace the conventional plasmonic materials with graphene for frequency-agile responses and it is of fundamental importance in extending the working frequency band of resonant metamaterials and metasurfaces; ii) the *kinetic inductance* is dominant with respect to the geometric inductance in the resonant graphene patterns, leading that graphene metasurfaces will operate at a deep-subwavelength scale, very well described as an effective medium avoiding periodicity artifacts;[40] iii) atomically thin graphene metasurfaces considerably strengthen the light-graphene interactions.

3.1. Tunable plasmonic resonances in graphene metasurfaces

The unusual graphene plasmon was theoretically studied for a new platform with strong light-matter interaction.[20] It is found that the graphene plasmons demonstrate much tighter confinement and longer propagating distances, and show the highly tunable feature via kinds of doping. Graphene sheets with nanometer-sized patterns including nanoribbons and nanodisks were found to yield further advantages, such as extreme field confinement in all-dimensions, plasmonic resonances engineering and increased coupling efficiency in optical fields. Long *et al.* experimentally demonstrated the tunable graphene plasmonic excitations in terahertz in engineered graphene ribbons.[50] It is demonstrated that by properly changing the width of micro-ribbons and applying in situ electrostatic doping, one is able to adjust graphene plasmon resonances over a broad terahertz frequency range. Plasmon excitations in the array of graphene micro-ribbons can be controlled via electrical gating for absorbing perpendicularly polarized light. Prominent plasmon absorption peaks are observed in experiments, and upon increasing carrier concentration, the resonances show a blue-shift in frequency with enhanced oscillation strength. It is also practicable to control plasmon excitations in graphene by engineering the geometric size of the ribbons. The top panel of **Figure 4a** displays AFM images of three different ribbon arrays with corresponding widths of 1, 2 and 4 μm, respectively, and the bottom panel of **Figure 4a** shows the spectra of gate-induced transmission decrease [$\Delta T = T - T_{CNT}$, T_{CNT} is the transmission coefficient at the charge neutral point] for the three structures. The plasmon resonance is observed to shift to higher energy while the ribbon width decreases. Therefore, by adjusting the width of nano- and micro-ribbons with a larger range, the resonance can be readily engineered in the whole terahertz regime.

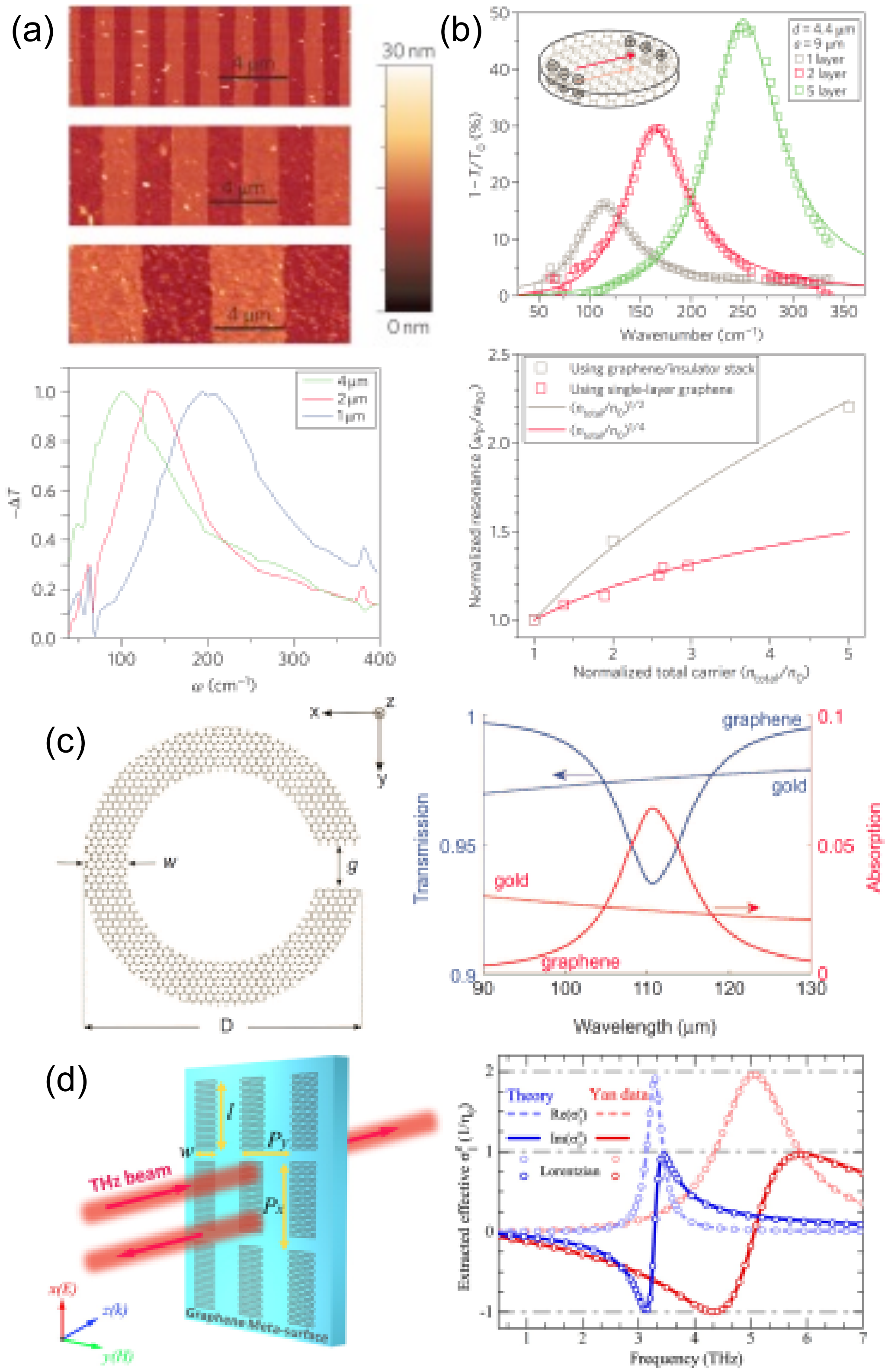

Figure 4. a) AFM images of samples with micro-ribbon widths of 1, 2 and 4 μm. Change of transmission spectra with different graphene micro-ribbon widths for the same doping concentration of 1.5× 10^{13} cm^{-2}. b) Extinction in transmission, 1-T/T_0, in stacked plasmonic devices with one, two and five graphene layers. Normalized plasmonic resonance frequency versus normalized total carrier density (bottom). c) A GSR resonator with diameter D, width W and gap distance g. (b) The normal-incidence transmittance (blue) and

absorbance (red) spectra of a square split ring array on monolayer graphene (solid curves). d) Schematic of the single-layer graphene cut-wire structure, and extracted effective surface conductivities for graphene cut wire arrays with different set of graphene data. a) Reproduced with permission.[50] Copyright 2011, Nature Publishing Group. b) Reproduced with permission.[56] Copyright 2012, Nature Publishing Group. c) Reproduced under a Creative Commons Attribution-NonCommercial-Share Alike 3.0 License.[43] Copyright 2013, Nature Publishing Group. d) Reproduced with permission.[91] Copyright 2015, American Chemical Society.

Multi-layered graphene microstructures were fabricated later by Yan *et al.* in graphene stacks, which were realized by alternatively depositing graphene and insulating layers.[56] They experimentally demonstrated that the plasmon in the stacked structures shows some non-classical features. Injecting carriers into multiple layers enhances the magnitude of resonance and significantly influences the frequency of plasmon resonance compared with the case of doping in single-layer graphene. This feature is different from conventional semiconductor superlattices. **Figure 4b** shows the extinction spectra for micro-disk arrays with different numbers of graphene layers. It indicates that densely-stacked graphene disks will lead to a drastic frequency shift of the plasmon resonance. The increased resonant frequency is beyond the description of classical models, but has to be interpreted in the scope of quantum mechanics, according to which, the graphene plasmon resonance of massless Dirac fermions is proportional to $\hbar^{-1/2}$.[125-126]

The aforementioned plasmonic resonances in micro-structured graphene sheets are all of electric dipolar modes. The magnetic response in graphene metasurface with SRRs was found to be rather weak.[39] **Figure 4c** shows a schematic graphene split ring (GSR) with the diameter of 1 μm. The study mainly focused on the case with *y*-axis polarized electric field under normal incidence. Such a configuration produces an electric dipole along the direction of the incident field and circulating current around the ring, which results in a magnetic dipole perpendicular to the ring (*z*-direction). The maximum coupling to the ring happens at the wavelength around 110 μm, which is much larger than the dimension of the ring, as indicated by the GSR resonance feature observed in the simulated transmission and absorption spectra of **Figure 4c** (right panel). Despite of the much smaller size compared to the excitation wavelength and the atomic thickness, the GSR-resonator metamaterial presents a clear resonant spectral feature with transmission declining to 94% while absorption reaching 6%. Both the fundamental magnetic and electric modes were excited by the introduction of asymmetry into the graphene SRR array,[38] and the contributions to the enhancement of infrared extinction and absorption of these two modes were comparatively studied. The magnetic resonance is rather weak represented by an extremely shallow dip in the transmission spectrum. In contrast, the electric mode responds to the incident field in a much stronger manner, showing higher extinction and absorption correspondingly.

As the simplest structure supporting electric dipolar mode, cut-wire plays an essential role in the design of plasmonic metamaterials. It has been extensively investigated toward the realization of various novel functionalities, such as plasmon-induced transparency, optical antennas and polarization manipulations. We studied the tunability of a metasurface made by a monolayer graphene patterned in the form of an array of cut-wire resonators in the terahertz regime (see **Figure 4d**).[91] Maximum absorption 50% was achieved under the electric dipolar mode. To characterize the graphene metasurface, we employed the sheet retrieval method [127], suitable for 2D systems, to calculate the effective electric surface conductivity from the complex scattering coefficients. In the view of the transfer matrix, the maximum absorption of the graphene metasurface would be 50%. When we applied two different sets of experimentally measured data of graphene (Li *et al.* data[30] and Yan *et al.* data[52]) to the graphene cut-wire metsurface, the calculations showed that the resonant response can be tuned and improved substantially in the terahertz regime. The tunable plasmonic resonances in graphene metasurfaces with various geometries have been intensively applied for significantly modulating the reflection, transmission, and absorption of light in the forms of plasmonically induced transparency (EIT) spectra and perfect absorbers.[87, 89, 128-140]

3.2. Functional light manipulations with complex 2D graphene metasurfaces

Fundamental electric and magnetic plasmonic resonances in patterned graphene sheets are the basic mechanism of various functional 2D metasurfaces. Based on the theoretical and experimental investigations on the basic graphene plasmonic resonances, various functional graphene-based 2D metasurfaces were proposed for exotic light manipulations in a tunable manner.

Lu *et al.* investigated the scattering properties of bi-ribbon graphene structures and found such a bi-ribbon unit will lead a large amplitude of scattering of the TM polarized wave with a wide phase range, potentially as a good candidate for the wave-front control.[42] To demonstrate the feasibility of graphene nanoribbon metasurfaces, a flat lens was designed with controllable focal length showing anomalous refraction (see **Figure 5a**). The anomalous angle of refraction is about 8.2°, matching the designed value considerably well yet slightly smaller. Such a discrepancy is due to two factors. First, the graphene unit is not diffusive, and the light scattered by each unit has angular distribution. Second, the size effect of the device can also lead to a difference between simulated results and theoretical predictions based on geometric arguments, in which the device size is generally considered to be much larger than the wavelength. Cheng *et al.* demonstrated tunable broadband anomalous refractions of circularly polarized waves with a nano-cross graphene metasurface in the infrared regime.[43] The scheme was investigated at various angles of incidence and different wavelengths, showing anomalous refraction in a broad range of frequency and angle of incidence (**Figure 5b**). The anomalous refraction can also occur upon reversing the polarization of the incident light. In addition, it is possible to dynamically control the anomalous conversion efficiency, which can remain high within a broadband of frequency by only changing the Fermi energy, not necessary to re-optimize the structure for adjusting the resonant frequency.

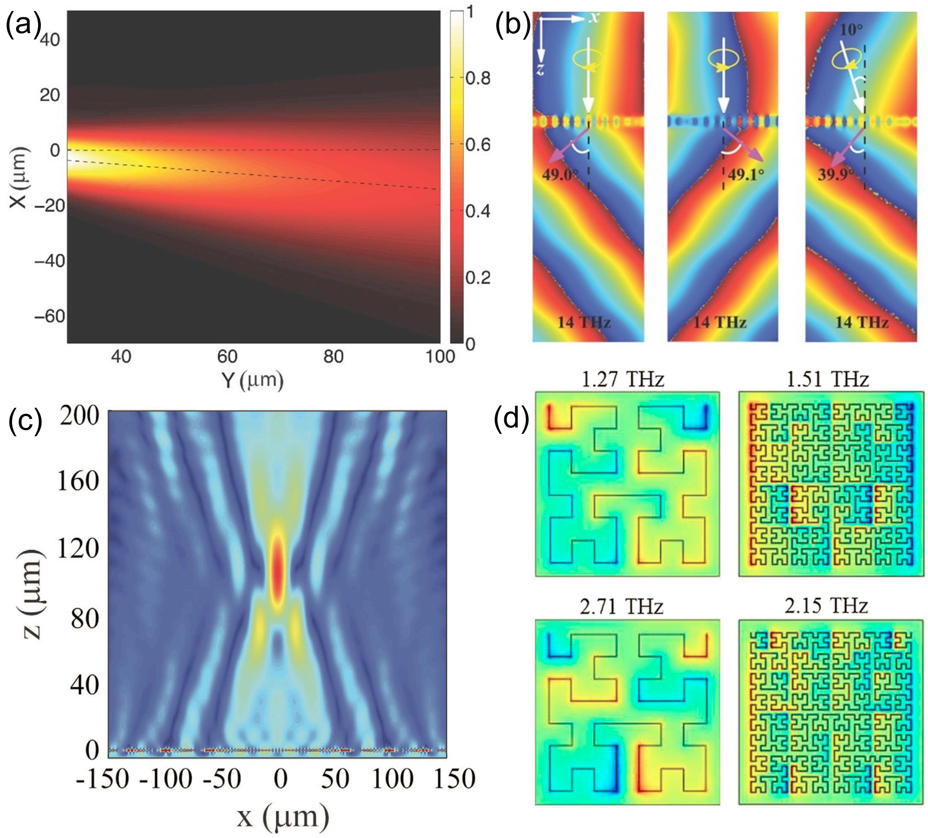

Figure 5. a) Simulated anomalous refraction. The tilted dashed line represents anomalous refractive angle of 8.2°. b) Simulated anomalous phase distributions of opposite handedness circular polarization: normally incident LCP wave (left), LCP wave (middle) and oblique incident LCP wave (incident angle: 10°, right). c) Dynamically tunable reflective focusing lens by varying the Fermi energy of graphene. Graphene ribbons are located at the plane of $z = 0$. d) The electromagnetic field maps for graphene Hilbert structures (of levels III and V) at two lowest-order resonances. a) Reproduced with permission.[42] Copyright 2014, Wiley-VCH. b) Reproduced with permission.[43] Copyright 2015, Wiley-VCH. c) Reproduced under a Creative Commons Attribution 4.0 International License.[90] Copyright 2015, Nature Publishing Group. d) Reproduced with permission. [47] Copyright 2016, American Physical Society.

Graphene metasurfaces with modulated geometries of ribbons were also exploited for efficiently steering infrared light with some reflective configuration.[90] Coupled with a subwavelength-thick optical cavity, the graphene ribbons were shown to achieve a near-2π phase modulation with high reflectivity. Anomalous reflection, reflective focusing lenses and non-diffracting beam generation with the capability of dynamic tuning were also demonstrated. **Figure 5c** presents the reflective focusing with the Fermi energy of graphene set to be 0.56 eV. The strategy of the design can be extended to far-infrared and mid-infrared frequencies by correspondingly adjusting the dimensions of graphene ribbons. Graphene-based metasurfaces could also be actively tuned for smart wavefront engineering in the reflective configuration.[141] In the study, graphene ribbons together with dielectric resonators were designed to cover a triangular bump for the demonstration of illusion optics, beam steering, and beam forming.

Properly designed more complex 2D patterns on graphene films, i.e. the 2D graphene metasurfaces could provide luxuriant functional light manipulations for diverse applications, including functionalities of polarization-independent, and strong polarization conversions etc. For instance, graphene metasurfaces with both positive and negative graphene Hilbert metasurfaces of levels from I to V were investigated throughout the terahertz and mid-infrared range.[47] It was shown that graphene fractal metasurfaces can exhibit a tunable and broadband absorption. Multiple resonances in the fractal graphene metasurface were designed for the broadband response in terahertz regime. **Figure 5d** shows the electromagnetic field maps for graphene Hilbert structures (of levels III and V) at two lowest-order resonances (from top to bottom).

4. 2D optics with graphene: Challenges and recent progresses

Despite the strong confinement to atomic scale of graphene plasmons together with the tunable optical properties of graphene have proved graphene a promising candidate in realizing tailorable functionalities for 2D optics, some critical challenges still exist in developing more efficient graphene-based 2D optical devices and systems. In this section, we will focus on some recent progresses including: i) The photo-excitation in graphene which can be employed to compensate the intrinsic loss in graphene metasurfaces so as to achieve high performance light manipulations. ii) Developed transformation optics links the 2D graphene metasurface to 3D geometry. This strategy can be employed for efficiently designing graphene plasmon-based 2D functionalities in analogy to 3D optics.

4.1. Photo-excited graphene metasurfaces

Even though graphene is promising in realizing tailorable functionalities in 2D optical circuits and 2D metasurfaces. The intrinsic loss in graphene would hamper many practical applications of its 2D plasmonic excitations. The real-part of the surface conductivity, representing the intrinsic loss of graphene, is fairly large, leading to a quick decay of the propagating plasmons and weak excitations of local resonant plasmonic modes.[38-40, 142] This is in fact similar to the conventional metallic plasmonic metamaterials, where the enhanced energy dissipation in metamaterials caused by the resonant nature of meta-atoms and the intrinsic loss of metals obstruct them from an efficient manipulation to the flow of light. Many studies have been carried out to reduce optical losses in metal-based metamaterials, such as avoiding sharp edges in the structure design,[143] and introducing low-loss metal like superconductors into metamaterials.[144-147] Incorporating active medium into metamaterials offers a more efficient and straightforward approach to solve the issue of losses.[148] Many experimental and theoretical works in recent years have shown loss compensation can lead to high-quality optical metamaterials via quantum dots, quantum wells and dyes.[149-153]

The unique band structure of graphene allows the possibility of a new mechanism for loss compensation. The gapless and linear dispersion of the 2D Dirac Fermions can have negative dynamic conductivity in an ultra-wide frequency range with optical pumping.[154-159] The stimulated emission in graphene in the regimes of terahertz and near-infrared has been experimentally demonstrated with inverted Dirac fermion population through time-resolved spectroscopy of fast non-equilibrium carrier relaxation dynamics. The stimulated emissions in photo-excited graphene make graphene an excellent candidate for active photonic applications.

The photo-excited graphene was involved in a metasurface for designing a ***PT***-symmetric system in the terahertz regime. As shown in **Figure 6a**, These graphene metasurface and metal sheets are separated by a dielectric gap. A graphene metasurface with optical pumping may exhibit a negative surface resistance in the terahertz regime, as opposed to that of metallic filament. The paired loss and gain sheets can effectively realize the ***PT***-symmetric system,[160] and the geometry of the graphene metasurface was properly designed to balance the loss of a resistive metallic filament in the vicinity of the exceptional point. The photoexcited graphene metasurface based ***PT***-symmetric system was suggested for sensing by taking advantage of the quite narrow eigenvalue bifurcation band. The existence of a ***PT***-symmetric or -broken transition is very sensitive to n- or p-type surface adsorbates in graphene metasurfaces. The unidirectional scatterings of the proposed ***PT***-symmetric system operated at the exceptional point can be chemically sensitive (see the bottom panel of **Figure. 6a**).

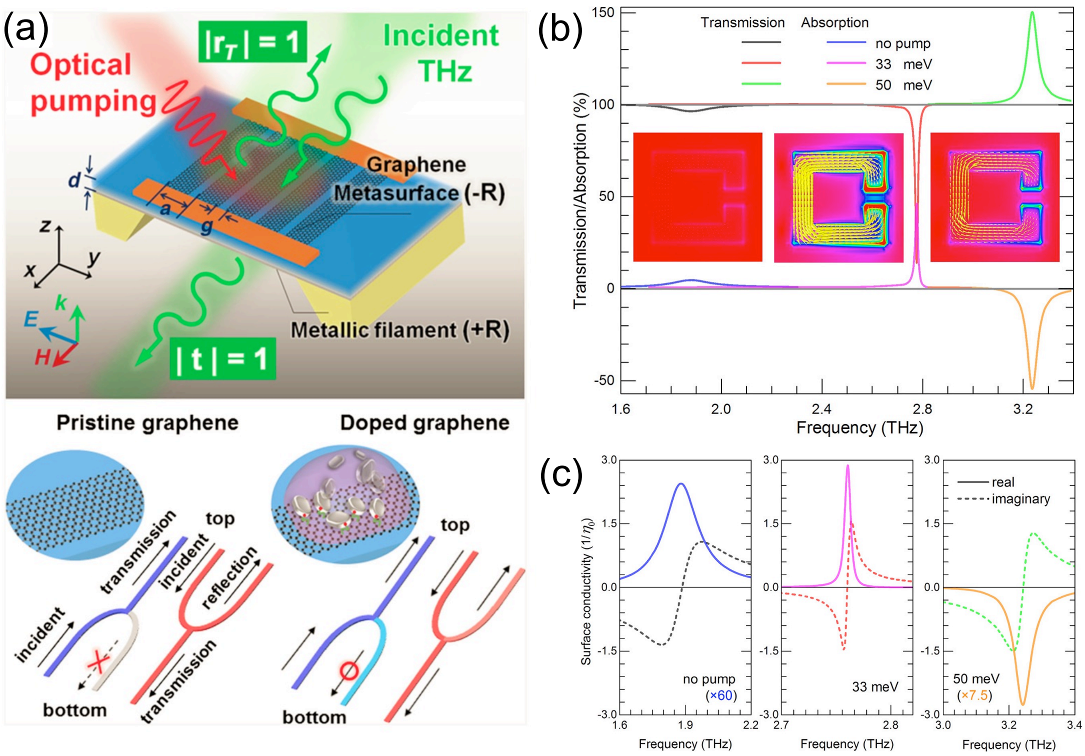

Figure 6. a) Top panel: Schematic integration of a *PT*-symmetric THz system consisting of an active graphene metasurface and an absorbing metallic sheet. Bottom panel: Illustration of the transmission and reflection of THz waves incident from the bottom (outlined as blue) and top (outlined as red) of a graphene-based PT-symmetric sensor, before (left) and after (right) being chemically doped. b) Magnetic resonances of photoexcited graphene metasurfaces with different quasi-Fermi levels at 300K. The transmission and absorption spectra are shown for unpumped graphene, pumped graphene with quasi-Fermi levels of 33 meV and 50 meV, respectively. The on-resonance local field and surface current maps (under same display setting) are plotted in the middle accordingly. c) Extracted surface conductivities for photoexcited graphene metasurfaces with different quasi-Fermi levels at 300 K (corresponding to the cases

in Figure 6b). a) Reproduced with permission.[94] Copyright 2016, American Physical Society. b-c) Reproduced with permission.[142] Copyright 2018, American Chemical Society.

The negative dynamic conductivity in the photo-excited graphene was also employed in metasurfaces for boosting the plasmonic excitations, specifically the weakly excited magnetic resonance.[38-40] A monolayer photo-excited graphene is patterned into an SRR array, a most common magnetic structure in metasurface designs. The terahertz scattering of the photo-excited graphene metasurfaces was investigated at both 77 K (liquid nitrogen temperature) and 300 K (room temperature).[142] Upon increasing the excitation power of the pump beam, the on-resonance transmission experiences a strong modulation from nearly unit to the minimum value around 8%, then shows an increment reversely, and finally the photo-excited graphene metasurface becomes lasing with an amplified beam propagating through the SRRs. The modulation and tunability are generally the same for both temperatures. **Figure 6b** presents the case at 300 K for unpumped graphene, and pumped graphene with quasi-Fermi levels of 33 meV and 50 meV, respectively. A sheet retrieval method was employed to extract the effective surface conductivity for the 300 K case, the extracted surface conductivities with both the real and imaginary parts for photo-excited graphene metasurfaces with different quasi-Fermi levels at 300 K are presented in **Figure 6c** (corresponding to **Figure 6b**). With the quasi-Fermi level being 33 meV, the surface conductivity is 60 times larger than that of the unpumped case, and the Lorentz resonance becomes much stronger. When the qausi-Fermi level increases to 50 meV, the extracted real-part of the conductivity becomes negative, suggesting the graphene metasurface is photo-excited to be active. The analysis with effective conductivity confirms quantitatively that the resonance of graphene metasurface can be boosted efficiently under photo-excitations.

4.2. Transformation optics links 2D optics and bulk optics with singularity

To date, most of the graphene plasmonic structures were designed based on the specific dispersion characteristic of propagating surface plasmonics and locally resonant graphene plasmonics. These methods are relatively inefficient and not straightforward. Therefore, more general and straightforward method is highly desirable for the design of 2D functional optics. Recently, Pendry *et al.* proposed a strategy to reduce a dimension through a singular transformation which can compress one of the dimensions of a 3D system into one or more singular points.[161] The compression of 3D plasmonic structure can be realized by employing the transformation optics, which exploits the invariance of Maxwell's equations via transforming the coordinates.[162-164] Taking a periodic metallic slab supporting surface plasmons as an example, the 3D plasmonic structure is transformed to a singular grating by exploiting a series of 2D conformal transformations. Then, a doped graphene layer is linked to the singular grating with a further step of conformal transformation. The singular grating can be modeled by increasing the modulation on the doped graphene layer till the electron density and the conductivity approach zero at a singular point.

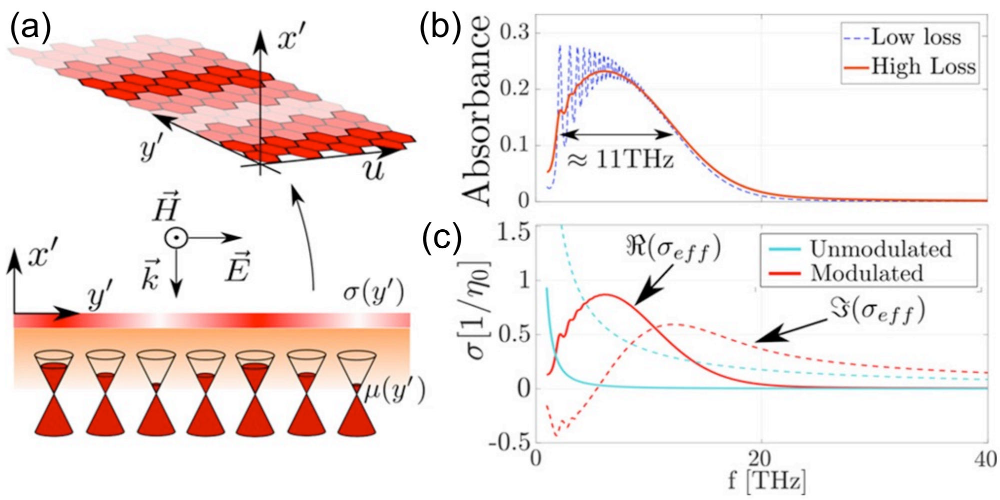

Figure 7. a) Graphene metasurface with periodically modulated conductivity. Conformal transformations are used to model a graphene sheet with periodically modulated doping level. b) Effect of losses in the spectrum of singular graphene metasurfaces, demonstrating how the peaks are completely merged into a continuum once the resistive broadening reaches the spacing between the modes. Absorbance is shown for the two most singular metasurfaces for different values of losses. The full bandwidth at half-maximum is ≈11.1 THz. c) The real (solid lines) and imaginary (dashed lines) parts of the effective conductivity (red lines) as well as the original, homogeneous graphene conductivity (light blue lines) in the singular limit. Reproduced with permission.[165] Copyright 2018, American Chemical Society.

The transformation-optics approach was later applied for designing graphene metasurfaces with broadband and tunable terahertz absorption.[165] A graphene layer with modulations on surface conductivity along one dimension of the surface as well as in frequency domain, is shown physically equivalent to a singular grating with broadband absorption under the conformal transformations, as shown in **Figure 7a**. The model system described an exotic phenomenon with a compacted dimension.[161] The hidden dimension significantly influences electromagnetic properties of the system: Transmission through a single sheet of graphene structure with our prescription shows a broadband strong absorption of terahertz radiation, which is opposed to isolated absorption peaks of a conventional grating. There exists a discrete series of absorption peaks, which are well separated in spectrum, for the least singular cases. When the weight of the plasmon is drawn into the singularity, the coupling to the external field is reduced. Thus, more peaks are visible in the absorption. Multiple surface plasmonic resonances merge into a continuum of modes when one approaches the singular limit as can be seen from **Figure 7b** (the corresponding modulated spectrum of conductivity is presented in **Figure 7c**). Higher losses in graphene layer will lead to a complete smearing of the spectrum, and will therefore merge the discrete peaks into a continuum. The technique of transformation optics was recently employed to derive the optical spectra of continuous graphene sheets by modulating local conductivity periodically via covering sinusoidal dielectric metasurfaces and achieve an efficient coupling of light into plasmons.[166]

5. Conclusion and Outlook

Manipulating light with graphene plasmon is an important way to realize deep subwavelength devices and systems for 2D optics. Progresses in the field include 2D optical circuits based on freely controlled propagating on the single layer carbon atoms, and 2D graphene metasurfaces with selectively excited and tailored plasmonic resonances in structured graphene layers. It was shown that the 2D optical platform based on graphene plasmon excitations can be exploited for effective and smart manipulation of light in a wide spectrum. We also discussed some new developments, such as photoexcited graphene metasurfaces and developed transformation optics linking 2D optics to bulk optics with singularity, which may be taken to overcome the obstacles towards practical 2D optics. We note that the current work mainly focused on the 2D optics based on monolayer graphene due to space restrictions. There has been some interesting work recently regarding stacked graphene,[167-170] for example, magneto-electric effect can be acquired by twisting two graphene layers. It was experimentally shown that remarkably strong circular dichroism can be structurally controlled with a two-atom-thick chiral film.[167] Furthermore, graphene plasmonic polariton is just a specific case of polaritons, the concept of 2D optics and its potential applications can also apply to other 2D phonon and exciton polaritons. Various two-dimensional materials beyond graphene can be similarly employed for 2D optics, and the related topic might be devoted in more specific literature.[171-172]

Acknowledgements

The authors would like to acknowledge financial support from the National Science Foundation of China (NSFC) (Grants Nos. 11674266, 61505164, 61771402, 51575297, 11774057, 11674248), the Science and Technology Plan of Shenzhen City (JCYJ20170817162221169), and the Fundamental Research Funds for the Central Universities (Grants Nos. 3102017zy033, 3102018jgc008). Work at Ames Laboratory was partially supported by the U.S. Department of Energy, Office of Basic Energy Science, Division of Materials Science and Engineering (Ames Laboratory is operated for the U.S. Department of Energy by Iowa State University under contract No. DE-AC02-07CH11358). The European Research Council under the ERC Advanced Grant No. 320081 (PHOTOMETA) supported work (theory) at FORTH.

Received: ((will be filled in by the editorial staff))
Revised: ((will be filled in by the editorial staff))
Published online: ((will be filled in by the editorial staff))

References

[1] A. K. Geim, K. S. Novoselov, *Nat. Mater.* **2007**, 6, 183.
[2] A. H. Castro Neto, F. Guinea, N. M. R. Peres, K. S. Novoselov, A. K. Geim, *Rev. Mod. Phys.* **2009**, 81, 109.
[3] A. K. Geim, *Science* **2009**, 324, 1530.
[4] F. Bonaccorso, Z. Sun, T. Hasan, A. C. Ferrari, *Nat. Photonics* **2010**, 4, 611.
[5] F. J. García de Abajo, *ACS Photonics* **2014**, 1, 135.
[6] S. Z. Butler, S. M. Hollen, L. Cao, Y. Cui, J. A. Gupta, H. R. Gutiérrez, T. F. Heinz, S. S. Hong, J. Huang, A. F. Ismach, E. Johnston-Halperin, M. Kuno, V. V. Plashnitsa, R. D. Robinson, R. S. Ruoff, S. Salahuddin, J. Shan, L. Shi, M. G. Spencer, M. Terrones, W. Windl, J. E. Goldberger, *ACS Nano* **2013**, 7, 2898.
[7] G. Fiori, F. Bonaccorso, G. Iannaccone, T. Palacios, D. Neumaier, A. Seabaugh, S. K. Banerjee, L. Colombo, *Nat. Nanotechnol.* **2014**, 9, 768.
[8] F. Xia, H. Wang, D. Xiao, M. Dubey, A. Ramasubramaniam, *Nat. Photonics* **2014**, 8, 899.
[9] K. S. Novoselov, A. K. Geim, S. V. Morozov, D. Jiang, Y. Zhang, S. V. Dubonos, I. V. Grigorieva, A. A. Firsov, *Science* **2004**, 306, 666.
[10] C. Lee, X. Wei, J. W. Kysar, J. Hone, *Science* **2008**, 321, 385.
[11] S. V. Morozov, K. S. Novoselov, M. I. Katsnelson, F. Schedin, D. C. Elias, J. A. Jaszczak, A. K. Geim, *Phys. Rev. Lett.* **2008**, 100, 016602.
[12] A. A. Balandin, S. Ghosh, W. Bao, I. Calizo, D. Teweldebrhan, F. Miao, C. N. Lau, *Nano Lett.* **2008**, 8, 902.
[13] F. J. García de Abajo, *Science* **2013**, 339, 917.
[14] P. Tassin, T. Koschny, C. M. Soukoulis, *Science* **2013**, 341, 620.
[15] T. Low, P. Avouris, *ACS Nano* **2014**, 8, 1086.
[16] Q. Bao, K. P. Loh, *ACS Nano* **2012**, 6, 3677.
[17] S. Chakraborty, O. P. Marshall, T. G. Folland, Y.-J. Kim, A. N. Grigorenko, K. S. Novoselov, *Science* **2016**, 351, 246.
[18] M. Jablan, H. Buljan, M. Soljačić, *Phys. Rev. B* **2009**, 80, 245435.
[19] S. A. Mikhailov, K. Ziegler, *Phys. Rev. Lett.* **2007**, 99, 016803.
[20] F. H. L. Koppens, D. E. Chang, F. J. García de Abajo, *Nano Lett.* **2011**, 11, 3370.
[21] Z. Fei, A. S. Rodin, G. O. Andreev, W. Bao, A. S. McLeod, M. Wagner, L. M. Zhang, Z. Zhao, M. Thiemens, G. Dominguez, M. M. Fogler, A. H. C. Neto, C. N. Lau, F. Keilmann, D. N. Basov, *Nature* **2012**, 487, 82.
[22] J. Chen, M. Badioli, P. Alonso-Gonzalez, S. Thongrattanasiri, F. Huth, J. Osmond, M. Spasenovic, A. Centeno, A. Pesquera, P. Godignon, A. Zurutuza Elorza, N. Camara, F. J. García de Abajo, R. Hillenbrand, F. H. L. Koppens, *Nature* **2012**, 487, 77.
[23] J. A. Gerber, S. Berweger, B. T. O'Callahan, M. B. Raschke, *Phys. Rev. Lett.* **2014**, 113, 055502.
[24] A. N. Grigorenko, M. Polini, K. S. Novoselov, *Nat. Photonics* **2012**, 6, 749.
[25] C. M. Soukoulis, T. Koschny, P. Tassin, N.-H. Shen, B. Dastmalchi, *Nanophotonics* **2015**, 4, 69.

[26] P. Zhang, N.-H. Shen, T. Koschny, C. M. Soukoulis, *ACS Photonics* **2017**, 4, 181.
[27] T. Christensen, W. Wang, A.-P. Jauho, M. Wubs, N. A. Mortensen, *Phys. Rev. B* **2014**, 90, 241414.
[28] A. Fallahi, T. Low, M. Tamagnone, J. Perruisseau-Carrier, *Phys. Rev. B* **2015**, 91, 121405.
[29] J. Chen, M. L. Nesterov, A. Y. Nikitin, S. Thongrattanasiri, P. Alonso-González, T. M. Slipchenko, F. Speck, M. Ostler, T. Seyller, I. Crassee, F. H. L. Koppens, L. Martin-Moreno, F. J. García de Abajo, A. B. Kuzmenko, R. Hillenbrand, *Nano Lett.* **2013**, 13, 6210.
[30] Z. Q. Li, E. A. Henriksen, Z. Jiang, Z. Hao, M. C. Martin, P. Kim, H. L. Stormer, D. N. Basov, *Nat Phys* **2008**, 4, 532.
[31] F. Wang, Y. Zhang, C. Tian, C. Girit, A. Zettl, M. Crommie, Y. R. Shen, *Science* **2008**, 320, 206.
[32] A. Vakil, N. Engheta, *Science* **2011**, 332, 1291.
[33] J. Horng, C.-F. Chen, B. Geng, C. Girit, Y. Zhang, Z. Hao, H. A. Bechtel, M. Martin, A. Zettl, M. F. Crommie, Y. R. Shen, F. Wang, *Phys. Rev. B* **2011**, 83, 165113.
[34] S. Thongrattanasiri, F. H. L. Koppens, F. J. García de Abajo, *Phys. Rev. Lett.* **2012**, 108, 047401.
[35] E. Carrasco, M. Tamagnone, J. Perruisseau-Carrier, *Appl. Phys. Lett.* **2013**, 102, 104103.
[36] P. Y. Chen, A. Alù, *IEEE Trans. Terahertz Sci. Technol.* **2013**, 3, 748.
[37] S. H. Mousavi, I. Kholmanov, K. B. Alici, D. Purtseladze, N. Arju, K. Tatar, D. Y. Fozdar, J. W. Suk, Y. Hao, A. B. Khanikaev, R. S. Ruoff, G. Shvets, *Nano Lett.* **2013**, 13, 1111.
[38] Y. Fan, Z. Wei, Z. Zhang, H. Li, *Opt. Lett.* **2013**, 38, 5410.
[39] N. Papasimakis, S. Thongrattanasiri, N. I. Zheludev, F. J. García de Abajo, *Light: Sci. Appl.* **2013**, 2, e78.
[40] N.-H. Shen, P. Tassin, T. Koschny, C. M. Soukoulis, *Phys. Rev. B* **2014**, 90, 115437.
[41] Y. Yao, R. Shankar, M. A. Kats, Y. Song, J. Kong, M. Loncar, F. Capasso, *Nano Lett.* **2014**, 14, 6526.
[42] F. Lu, B. Liu, S. Shen, *Adv. Opt. Mater.* **2014**, 2, 794.
[43] H. Cheng, S. Chen, P. Yu, W. Liu, Z. Li, J. Li, B. Xie, J. Tian, *Adv. Opt. Mater.* **2015**, 3, 1744.
[44] J. Li, P. Yu, H. Cheng, W. Liu, Z. Li, B. Xie, S. Chen, J. Tian, *Adv. Opt. Mater.* **2015**, 4, 91.
[45] P. A. Huidobro, M. Kraft, S. A. Maier, J. B. Pendry, *ACS Nano* **2016**, 10, 5499.
[46] V. Dmitriev, C. Nascimento, S. Prosvirnin, *IEEE Trans. Antennas Propag.* **2015**, 63, 5893.
[47] P. C. Wu, N. Papasimakis, D. P. Tsai, *Physical Review Applied* **2016**, 6, 044019.
[48] Z. Wu, W. Li, N. Yogeesh Maruthi, S. Jung, L. Lee Alvin, K. McNicholas, A. Briggs, R. Bank Seth, A. Belkin Mikhail, D. Akinwande, Y. Zheng, *Adv. Opt. Mater.* **2016**, 4, 2035.
[49] T. T. Kim, H. Kim, M. Kenney, S. Park Hyun, H. D. Kim, B. Min, S. Zhang, *Adv. Opt. Mater.* **2018**, 6, 1700507.
[50] L. Ju, B. Geng, J. Horng, C. Girit, M. Martin, Z. Hao, H. A. Bechtel, X. Liang, A. Zettl, Y. R. Shen, F. Wang, *Nat. Nanotechnol.* **2011**, 6, 630.
[51] V. W. Brar, M. S. Jang, M. Sherrott, J. J. Lopez, H. A. Atwater, *Nano Lett.* **2013**, 13, 2541.
[52] H. Yan, T. Low, W. Zhu, Y. Wu, M. Freitag, X. Li, F. Guinea, P. Avouris, F. Xia, *Nat. Photonics* **2013**, 7, 394.

[53] Z. Fang, S. Thongrattanasiri, A. Schlather, Z. Liu, L. Ma, Y. Wang, P. M. Ajayan, P. Nordlander, N. J. Halas, F. J. García de Abajo, *ACS Nano* **2013**, 7, 2388.
[54] D. Rodrigo, O. Limaj, D. Janner, D. Etezadi, F. J. García de Abajo, V. Pruneri, H. Altug, *Science* **2015**, 349, 165.
[55] H. Hu, X. Yang, F. Zhai, D. Hu, R. Liu, K. Liu, Z. Sun, Q. Dai, *Nat. Commun.* **2016**, 7, 12334.
[56] H. Yan, X. Li, B. Chandra, G. Tulevski, Y. Wu, M. Freitag, W. Zhu, P. Avouris, F. Xia, *Nat. Nanotechnol.* **2012**, 7, 330.
[57] M. Kauranen, A. V. Zayats, *Nat. Photonics* **2012**, 6, 737.
[58] X. Zhao, C. Yuan, L. Zhu, J. Yao, *Nanoscale* **2016**, 8, 15273.
[59] G. Yao, F. Ling, J. Yue, C. Luo, J. Ji, J. Yao, *Opt. Express* **2016**, 24, 1518.
[60] D. R. Smith, J. B. Pendry, M. C. K. Wiltshire, *Science* **2004**, 305, 788.
[61] N. Liu, H. Guo, L. Fu, S. Kaiser, H. Schweizer, H. Giessen, *Nat. Mater.* **2007**, 7, 31.
[62] C. M. Soukoulis, M. Wegener, *Nat. Photonics* **2011**, 5, 523.
[63] E. Plum, X. X. Liu, V. A. Fedotov, Y. Chen, D. P. Tsai, N. I. Zheludev, *Phys. Rev. Lett.* **2009**, 102, 113902.
[64] T. Kaelberer, V. A. Fedotov, N. Papasimakis, D. P. Tsai, N. I. Zheludev, *Science* **2010**, 330, 1510.
[65] A. E. Nikolaenko, F. De Angelis, S. A. Boden, N. Papasimakis, P. Ashburn, E. Di Fabrizio, N. I. Zheludev, *Phys. Rev. Lett.* **2010**, 104, 153902.
[66] Q. Zhao, L. Kang, B. Du, H. Zhao, Q. Xie, X. Huang, B. Li, J. Zhou, L. Li, *Phys. Rev. Lett.* **2008**, 101, 027402.
[67] F. Zhang, Q. Zhao, L. Kang, J. Zhou, D. Lippens, *Phys. Rev. B* **2009**, 80, 195119.
[68] Z. Wei, Y. Cao, J. Han, C. Wu, Y. Fan, H. Li, *Appl. Phys. Lett.* **2010**, 97, 141901.
[69] J. Han, H. Li, Y. Fan, Z. Wei, C. Wu, Y. Cao, X. Yu, F. Li, Z. Wang, *Appl. Phys. Lett.* **2011**, 98, 151908.
[70] F. Zhang, S. Feng, K. Qiu, Z. Liu, Y. Fan, W. Zhang, Q. Zhao, J. Zhou, *Appl. Phys. Lett.* **2015**, 106, 091907.
[71] Q. Zhao, Z. Xiao, F. Zhang, J. Ma, M. Qiao, Y. Meng, C. Lan, B. Li, J. Zhou, P. Zhang, N. H. Shen, T. Koschny, C. M. Soukoulis, *Adv. Mater.* **2015**, 27, 6187.
[72] R. Peng, Z. Xiao, Q. Zhao, F. Zhang, Y. Meng, B. Li, J. Zhou, Y. Fan, P. Zhang, N.-H. Shen, T. Koschny, C. M. Soukoulis, *Physical Review X* **2017**, 7, 011033.
[73] Y. Fan, F. Zhang, N.-H. Shen, Q. Fu, Z. Wei, H. Li, C. M. Soukoulis, *Phys. Rev. A* **2018**, 97, 033816.
[74] N. Yu, F. Capasso, *Nat. Mater.* **2014**, 13, 139.
[75] A. V. Kildishev, A. Boltasseva, V. M. Shalaev, *Science* **2013**, 339, 1232009.
[76] N. Yu, P. Genevet, M. A. Kats, F. Aieta, J.-P. Tetienne, F. Capasso, Z. Gaburro, *Science* **2011**, 334, 333.
[77] X. Ni, N. K. Emani, A. V. Kildishev, A. Boltasseva, V. M. Shalaev, *Science* **2012**, 335, 427.
[78] S. Sun, Q. He, S. Xiao, Q. Xu, X. Li, L. Zhou, *Nat. Mater.* **2012**, 11, 426.
[79] X. Yin, Z. Ye, J. Rho, Y. Wang, X. Zhang, *Science* **2013**, 339, 1405.
[80] N. Shitrit, I. Yulevich, E. Maguid, D. Ozeri, D. Veksler, V. Kleiner, E. Hasman, *Science* **2013**, 340, 724.
[81] C. Lu, X. Hu, K. Shi, Q. Hu, R. Zhu, H. Yang, Q. Gong, *Light: Sci. Appl.* **2015**, 4, e302.
[82] P.-Y. Chen, A. Alù, *ACS Nano* **2011**, 5, 5855.
[83] M. S. Jang, V. W. Brar, M. C. Sherrott, J. J. Lopez, L. Kim, S. Kim, M. Choi, H. A. Atwater, *Phys. Rev. B* **2014**, 90, 165409.
[84] J. Li, Y. Zhou, B. Quan, X. Pan, X. Xu, Z. Ren, F. Hu, H. Fan, M. Qi, J. Bai, L. Wang, J. Li, C. Gu, *Carbon* **2014**, 78, 102.

[85] Y. Zhang, Y. Feng, B. Zhu, J. Zhao, T. Jiang, *Opt. Express* **2014**, 22, 22743.
[86] W. Zhu, F. Xiao, M. Kang, D. Sikdar, M. Premaratne, *Appl. Phys. Lett.* **2014**, 104, 051902.
[87] Y. Fan, F. Zhang, Q. Zhao, Z. Wei, H. Li, *Opt. Lett.* **2014**, 39, 6269.
[88] S. Li, Q. Duan, S. Li, Q. Yin, W. Lu, L. Li, B. Gu, B. Hou, W. Wen, *Appl. Phys. Lett.* **2015**, 107, 181112.
[89] Y. Fan, Z. Liu, F. Zhang, Q. Zhao, Z. Wei, Q. Fu, J. Li, C. Gu, H. Li, *Sci. Rep.* **2015**, 5, 13956.
[90] Z. Li, K. Yao, F. Xia, S. Shen, J. Tian, Y. Liu, *Sci. Rep.* **2015**, 5, 12423.
[91] Y. Fan, N.-H. Shen, T. Koschny, C. M. Soukoulis, *ACS Photonics* **2015**, 2, 151.
[92] H. Lu, B. P. Cumming, M. Gu, *Opt. Lett.* **2015**, 40, 3647.
[93] Z. Miao, Q. Wu, X. Li, Q. He, K. Ding, Z. An, Y. Zhang, L. Zhou, *Physical Review X* **2015**, 5, 041027.
[94] P.-Y. Chen, J. Jung, *Phys. Rev. Appl.* **2016**, 5, 064018.
[95] S. C. Dhanabalan, J. S. Ponraj, H. Zhang, Q. Bao, *Nanoscale* **2016**, 8, 6410.
[96] Y. Fan, N.-H. Shen, F. Zhang, Z. Wei, H. Li, Q. Zhao, Q. Fu, P. Zhang, T. Koschny, C. M. Soukoulis, *Adv. Opt. Mater.* **2016**, 4, 1824.
[97] P. A. Huidobro, M. Kraft, R. Kun, S. A. Maier, J. B. Pendry, *J. Opt.* **2016**, 18, 044024.
[98] P. Arroyo Huidobro, S. A. Maier, J. B. Pendry, *EPJ Applied Metamaterials* **2017**, 4, 6.
[99] P.-Y. Chen, C. Argyropoulos, M. Farhat, J. S. Gomez-Diaz, *Nanophotonics* **2017**, 6, 1239.
[100] T.-T. Kim, S. S. Oh, H.-D. Kim, H. S. Park, O. Hess, B. Min, S. Zhang, *Sci. Adv.* **2017**, 3, e1701377.
[101] X. Liu, Z. Chen, E. P. J. Parrott, B. S. Y. Ung, J. Xu, E. Pickwell‐MacPherson, *Adv. Opt. Mater.* **2017**, 5, 1600697.
[102] Y. Fan, L. Tu, F. Zhang, Q. Fu, Z. Zhang, Z. Wei, H. Li, *Plasmonics* **2017**, DOI: 10.1007/s11468-017-0615-0doi: 10.1007/s11468.
[103] S. Kim, M. S. Jang, V. W. Brar, K. W. Mauser, L. Kim, H. A. Atwater, *Nano Lett.* **2018**, DOI: 10.1021/acs.nanolett.7b04393.
[104] T.-T. Kim, H.-D. Kim, R. Zhao, S. S. Oh, T. Ha, D. S. Chung, Y. H. Lee, B. Min, S. Zhang, *ACS Photonics* **2018**, 5, 1800.
[105] B. Wunsch, T. Stauber, F. Sols, F. Guinea, *New J. Phys.* **2006**, 8, 318.
[106] V. P. Gusynin, S. G. Sharapov, J. P. Carbotte, *J. Phys.: Condens. Matter* **2007**, 19, 026222.
[107] E. H. Hwang, S. Das Sarma, *Phys. Rev. B* **2007**, 75, 205418.
[108] G. W. Hanson, *J. Appl. Phys.* **2008**, 103, 064302.
[109] W. L. Barnes, A. Dereux, T. W. Ebbesen, *Nature* **2003**, 424, 824.
[110] E. Ozbay, *Science* **2006**, 311, 189.
[111] W. H. Backes, F. M. Peeters, F. Brosens, J. T. Devreese, *Phys. Rev. B* **1992**, 45, 8437.
[112] Y. Liu, R. F. Willis, K. V. Emtsev, T. Seyller, *Phys. Rev. B* **2008**, 78, 201403.
[113] S. Y. Shin, N. D. Kim, J. G. Kim, K. S. Kim, D. Y. Noh, K. S. Kim, J. W. Chung, *Appl. Phys. Lett.* **2011**, 99, 082110.
[114] A. Y. Nikitin, T. Low, L. Martin-Moreno, *Phys. Rev. B* **2014**, 90, 041407.
[115] F. Liu, C. Qian, Y. D. Chong, *Opt. Express* **2015**, 23, 2383.
[116] L. Wang, W. Cai, X. Zhang, J. Xu, Y. Luo, *Opt. Express* **2016**, 24, 19776.
[117] S. Vantasin, Y. Y. Tanaka, T. Shimura, *ACS Photonics* **2018**, 5, 1050.
[118] T. J. Constant, S. M. Hornett, D. E. Chang, E. Hendry, *Nat. Phys.* **2015**, 12, 124.
[119] G. X. Ni, A. S. McLeod, Z. Sun, L. Wang, L. Xiong, K. W. Post, S. S. Sunku, B. Y. Jiang, J. Hone, C. R. Dean, M. M. Fogler, D. N. Basov, *Nature* **2018**, 557, 530.
[120] D. N. Basov, in *2017 Annual Meeting of the APS Mid-Atlantic Section*, Newark, New Jersey 2018.

[121] P. Alonso-González, A. Y. Nikitin, Y. Gao, A. Woessner, M. B. Lundeberg, A. Principi, N. Forcellini, W. Yan, S. Vélez, A. J. Huber, K. Watanabe, T. Taniguchi, F. Casanova, L. E. Hueso, M. Polini, J. Hone, F. H. L. Koppens, R. Hillenbrand, *Nat. Nanotechnol.* **2016**, 12, 31.
[122] D. Alcaraz Iranzo, S. Nanot, E. J. C. Dias, I. Epstein, C. Peng, D. K. Efetov, M. B. Lundeberg, R. Parret, J. Osmond, J.-Y. Hong, J. Kong, D. R. Englund, N. M. R. Peres, F. H. L. Koppens, *Science* **2018**, 360, 291.
[123] J. S. Gomez-Diaz, M. Tymchenko, A. Alù, *Phys. Rev. Lett.* **2015**, 114, 233901.
[124] S. Inampudi, H. Mosallaei, *ACS Omega* **2016**, 1, 843.
[125] S. Das Sarma, E. H. Hwang, *Phys. Rev. Lett.* **2009**, 102, 206412.
[126] E. H. Hwang, S. Das Sarma, *Phys. Rev. B* **2009**, 80, 205405.
[127] P. Tassin, T. Koschny, C. M. Soukoulis, *Physica B* **2012**, 407, 4062.
[128] S.-X. Xia, X. Zhai, L.-L. Wang, B. Sun, J.-Q. Liu, S.-C. Wen, *Opt. Express* **2016**, 24, 17886.
[129] S.-X. Xia, X. Zhai, L.-L. Wang, S.-C. Wen, *Photon. Res.* **2018**, 6, 692.
[130] X. Shi, D. Han, Y. Dai, Z. Yu, Y. Sun, H. Chen, X. Liu, J. Zi, *Opt. Express* **2013**, 21, 28438.
[131] R. Alaee, M. Farhat, C. Rockstuhl, F. Lederer, *Opt. Express* **2012**, 20, 28017.
[132] A. Andryieuski, A. V. Lavrinenko, *Opt. Express* **2013**, 21, 9144.
[133] J. Zhang, C. Guo, K. Liu, Z. Zhu, W. Ye, X. Yuan, S. Qin, *Opt. Express* **2014**, 22, 12524.
[134] J. Ding, B. Arigong, H. Ren, M. Zhou, J. Shao, M. Lu, Y. Chai, Y. Lin, H. Zhang, *Sci. Rep.* **2014**, 4, 6128.
[135] Y. Zhang, T. Li, Q. Chen, H. Zhang, J. F. O'Hara, E. Abele, A. J. Taylor, H.-T. Chen, A. K. Azad, *Sci. Rep.* **2015**, 5, 18463.
[136] C. Zeng, Y. Cui, X. Liu, *Opt. Express* **2015**, 23, 545.
[137] L. Wang, W. Li, X. Jiang, *Opt. Lett.* **2015**, 40, 2325.
[138] Z. Zhang, Y. Fan, Y. Long, P. Yin, *Opt. Mater.* **2017**, 72, 632.
[139] S. Xiao, T. Wang, T. Liu, X. Yan, Z. Li, C. Xu, *Carbon* **2018**, 126, 271.
[140] S. J. Kindness, N. W. Almond, B. Wei, R. Wallis, W. Michailow, V. S. Kamboj, P. Braeuninger-Weimer, S. Hofmann, H. E. Beere, D. A. Ritchie, R. Degl'Innocenti, *Adv. Opt. Mater.* **2018**, 0, 1800570.
[141] S. R. Biswas, C. E. Gutiérrez, A. Nemilentsau, I.-H. Lee, S.-H. Oh, P. Avouris, T. Low, *Physical Review Applied* **2018**, 9, 034021.
[142] Y. Fan, N.-H. Shen, F. Zhang, Q. Zhao, Z. Wei, P. Zhang, J. Dong, Q. Fu, H. Li, C. M. Soukoulis, *ACS Photonics* **2018**, 5, 1612.
[143] D. Ö. Güney, T. Koschny, C. M. Soukoulis, *Phys. Rev. B* **2009**, 80, 125129.
[144] M. Ricci, N. Orloff, S. M. Anlage, *Appl. Phys. Lett.* **2005**, 87, 034102.
[145] H.-T. Chen, H. Yang, R. Singh, J. F. O'Hara, A. K. Azad, S. A. Trugman, Q. X. Jia, A. J. Taylor, *Phys. Rev. Lett.* **2010**, 105, 247402.
[146] V. Savinov, A. Tsiatmas, A. R. Buckingham, V. A. Fedotov, P. A. J. de Groot, N. I. Zheludev, *Sci. Rep.* **2012**, 2, 450.
[147] P. Tassin, T. Koschny, M. Kafesaki, C. M. Soukoulis, *Nat. Photonics* **2012**, 6, 259.
[148] C. M. Soukoulis, M. Wegener, *Science* **2010**, 330, 1633.
[149] E. Plum, V. A. Fedotov, P. Kuo, D. P. Tsai, N. I. Zheludev, *Opt. Express* **2009**, 17, 8548.
[150] A. Fang, T. Koschny, C. M. Soukoulis, *Phys. Rev. B* **2010**, 82, 121102.
[151] N. Meinzer, M. Ruther, S. Linden, C. M. Soukoulis, G. Khitrova, J. Hendrickson, J. D. Olitzky, H. M. Gibbs, M. Wegener, *Opt. Express* **2010**, 18, 24140.
[152] S. Wuestner, A. Pusch, K. L. Tsakmakidis, J. M. Hamm, O. Hess, *Phys. Rev. Lett.* **2010**, 105, 127401.

[153] S. Xiao, V. P. Drachev, A. V. Kildishev, X. Ni, U. K. Chettiar, H.-K. Yuan, V. M. Shalaev, *Nature* **2010**, 466, 735.
[154] V. Ryzhii, M. Ryzhii, T. Otsuji, *J. Appl. Phys.* **2007**, 101, 083114.
[155] S. Boubanga-Tombet, S. Chan, T. Watanabe, A. Satou, V. Ryzhii, T. Otsuji, *Phys. Rev. B* **2012**, 85, 035443.
[156] T. Li, L. Luo, M. Hupalo, J. Zhang, M. C. Tringides, J. Schmalian, J. Wang, *Phys. Rev. Lett.* **2012**, 108, 167401.
[157] V. V. Popov, O. V. Polischuk, S. A. Nikitov, V. Ryzhii, T. Otsuji, M. S. Shur, *J. Opt.* **2013**, 15, 114009.
[158] T. Otsuji, T. Watanabe, S. A. B. Tombet, A. Satou, W. M. Knap, V. V. Popov, M. Ryzhii, V. Ryzhii, *IEEE Trans. Terahertz Sci. Technol.* **2013**, 3, 63.
[159] D. Svintsov, V. Ryzhii, A. Satou, T. Otsuji, V. Vyurkov, *Opt. Express* **2014**, 22, 19873.
[160] R. Fleury, D. L. Sounas, A. Alù, *Phys. Rev. Lett.* **2014**, 113, 023903.
[161] J. B. Pendry, P. A. Huidobro, Y. Luo, E. Galiffi, *Science* **2017**, 358, 915.
[162] A. J. Ward, J. B. Pendry, *J. Mod. Opt.* **1996**, 43, 773.
[163] J. B. Pendry, D. Schurig, D. R. Smith, *Science* **2006**, 312, 1780.
[164] U. Leonhardt, *Science* **2006**, 312, 1777.
[165] E. Galiffi, J. B. Pendry, P. A. Huidobro, *ACS Nano* **2018**, 12, 1006.
[166] S. Xia, X. Zhai, Y. Huang, J. Liu, L. Wang, S. Wen, *Journal of Lightwave Technology* **2017**, 35, 4553.
[167] C.-J. Kim, A. Sánchez-Castillo, Z. Ziegler, Y. Ogawa, C. Noguez, J. Park, *Nat. Nanotechnol.* **2016**, 11, 520.
[168] T. Stauber, T. Low, G. Gómez-Santos, *Phys. Rev. Lett.* **2018**, 120, 046801.
[169] T. Low, P.-Y. Chen, D. N. Basov, *Phys. Rev. B* **2018**, 98, 041403.
[170] S. Kar, V. L. Nguyen, D. R. Mohapatra, Y. H. Lee, A. K. Sood, *ACS Nano* **2018**, 12, 1785.
[171] D. N. Basov, M. M. Fogler, F. J. García de Abajo, *Science* **2016**, 354.
[172] T. Low, A. Chaves, J. D. Caldwell, A. Kumar, N. X. Fang, P. Avouris, T. F. Heinz, F. Guinea, L. Martin-Moreno, F. Koppens, *Nat. Mater.* **2016**, 16, 182.